J Therm Anal Calorim (2012) 108:733–739
DOI 10.1007/s10973-011-2126-0

Study of the Cu–Li–Mg–H system by thermal analysis

M. H. Braga · J. A. Ferreira · M. J. Wolverton

MEDICTA2011 Conference Special Chapter

Abstract Finite fossil-fuel supplies, nuclear waste and global warming linked to CO_2 emissions have made the development of alternative/'green' methods of energy production, conversion and storage popular topics in today's energy-conscious society. These crucial environmental issues, together with the rapid advance and eagerness from the electric automotive industry have combined to make the development of radically improved energy storage systems a worldwide imperative. $CuMg_2$ has an orthorhombic crystal structure and does not form a hydride: it reacts reversibly with hydrogen to produce Cu_2Mg and MgH_2. However, $CuLi_xMg_{2-x}$ ($x = 0.08$) has a hexagonal crystal structure, just like $NiMg_2$, a compound known for its hydrogen storage properties. $NiMg_2$ absorbs up to 3.6 wt% of H. Our studies showed that not only $CuLi_xMg_{2-x}$ absorbs a considerable amount of hydrogen, but also starts releasing it at a temperature in the range of 40–130 °C. In order to determine the properties of the hydrogenated $CuLi_xMg_{2-x}$, absorption–desorption, Differential scanning calorimeter and thermogravimetric experiments were performed. Neutron spectra were collected to elucidate the behavior of hydrogen in the Li-doped $CuMg_2$ intermetallic. Using DFT calculations we were able to determine the best value for x in $CuLi_xMg_{2-x}$ and compare different possible structures for the $CuLi_xMg_{2-x}$ hydride.

M. H. Braga (✉)
CEMUC, Engineering Physics Department, Engineering Faculty, Porto University, R. Dr. Roberto Frias s/n, 4200-465 Porto, Portugal
e-mail: mbraga@fe.up.pt

M. H. Braga · M. J. Wolverton
Los Alamos National Laboratory (LANSCE), Los Alamos, NM 87545, USA

J. A. Ferreira
Laboratorio Nacional de Energia e Geologia, Rua da Amieira, Apartado 1089, 466-901 S. Mamede de Infesta, Portugal

Keywords DSC/TG · INS · Mg based alloys · Energy storage · Hydrides

Introduction

Efficient hydrogen storage remains a major technological obstacle toward the development of a hydrogen-based energy economy. Electric and hybrid vehicles use metal hydrides as the negative electrode (instead of cadmium) in their batteries [1, 2]. In fact, metal hydrides are widely used in consumer electronics rechargeable batteries. In Ni–MH, M is an intermetallic compound. The most common one has the AB_5 type, where A is a rare-earth mixture (e.g., La, Ce, Nd, Pr) and B is Ni, Co, Mn, and/or Al. Note that $LaNi_5H_6$, which is commonly used in batteries, stores only a maximum of 1.4 wt% of H. Another disadvantage of these materials for hydrogen storage is that lanthanides tend to be expensive and heavy.

We are currently investigating the Cu–Li–Mg–H system. The lighter and cheaper metals and our recent discovery that hydrogen can be reversibly stored in these compounds make them a very attractive alternative to lanthanide-based systems.

$CuMg_2$ has an orthorhombic crystal structure and does not form a hydride: it reacts reversibly with hydrogen to produce Cu_2Mg and MgH_2 [3]. However, $CuLi_xMg_{2-x}$ ($x = 0.08$) has a hexagonal crystal structure [4] (ICSD database [5]), just like $NiMg_2$, a compound known for its hydrogen storage properties. $NiMg_2$ absorbs up to 3.6 wt% H (of the hydride's weight) [6]. In spite of the fact that the percentage of hydrogen absorbed by $NiMg_2$ is enough to propitiate practical applications, the temperature at which the alloy desorbs hydrogen (282 °C (555 K) at 1 bar) is much too high for practical applications.

A comparison between the phase diagrams of the systems Cu–Mg and Ni–Mg shows that these binary systems form compounds with similar stoichiometry. $NiMg_2$ is formed by peritectic reaction of the elements at 759 °C (1,032 K) and $CuMg_2$ by congruent melting at 568 °C (841 K). The presence of Li lowers even further the melting point of $CuMg_2$ [7].

Since the enthalpy of formation of the hydride is related to that of the primary alloy [8], it was hypothesized that $CuLi_xMg_{2-x}$ might also be a hydrogen storage material similar to $NiMg_2$ [9]. Presumably, its advantage would be that it would release hydrogen at a lower temperature (possibly close to room temperature) [10].

Preliminary studies at the Los Alamos Neutron Scattering Center (LANSCE) showed that hydrogen unsaturated samples could desorb up to 4.4–5.3 wt% of hydrogen. Experiments furthermore shown that samples containing $CuLi_xMg_{2-x}$ will start desorbing hydrogen at a temperature from 40–130 °C where applications are easier to develop. Hence it should be possible to use this alloy with fuel cells or in batteries and hydrogen storage devices.

Sample preparation

The Cu–Li–Mg samples were prepared from the pure elements with a target composition of $CuLi_{0.1}Mg_{1.9}$. They were prepared by mixing stoichiometric amounts of Cu (electrolytic, 99.99% purity, 325 mesh), Mg (99.8% purity, 200 mesh, Alfa Aesar), and granules (approx. 2 × 2 × 3 mm) of Li (99% purity, Alfa Aesar). Because of the large vapour pressure of Mg, even below its melting point, the reagents were sealed in a stainless steel crucible in a dry box (He atmosphere). This eliminated possible reagent loss. The samples were heated in a tube furnace with a stirring device to ensure proper mixing of the heterogeneous starting mixture and complete dispersion of Li in the sample. Different reaction temperatures and times were used (from 450 °C for 24 h to 1,200 °C for 1–2 h). Regardless of reaction conditions, the samples invariably contained Cu_2Mg, $CuMg_2$, or both. Nonetheless, we obtained final products containing up to 82.5 at% (77.5 wt%) of $CuLi_xMg_{2-x}$. Since the structure of Cu_2Mg and $CuMg_2$ is known as well as their hydrogen storage behaviour; this complication translated merely in the refinement of additional phases in the neutron/X-ray powder diffraction patterns.

Samples were firstly characterized by means of X-ray diffraction (XRD) using a Rigaku Ultima III powder diffractometer, and their composition was roughly determined by means of the Match software, [11] which uses the "Reference Intensity Ratio method" RiR method) [12] to obtain phase fractions. Patterns were collected with CuK-alpha radiation with 2θ typically from 15° to 70° with steps of 0.02° and a counting time of 10 s per bin.

Hydrogen absorption experiments

A sample with approx. 74 at% of $CuLi_{0.08}Mg_{2-0.08}$, 20 at% of $CuMg_2$ and 6 at% of Cu_2Mg was grinded to obtain a powder with particle size of the order of 37 μm. The sample was then studied in a HPVA high pressure absorption analyser [13]. The latter gas adsorption analysers are designed to obtain high pressure adsorption isotherms of gases, such as hydrogen, using the static volumetric method. Two additional samples with –79 at% of $CuLi_{0.08}Mg_{1.92}$ and 21 at% of Cu_2Mg and –57 at% of $CuLi_{0.08}Mg_{1.92}$, 34 at% of $CuMg_2$ and 9 at% of Cu_2Mg– were measured too, to determine H_2 equilibrium pressure at different temperatures during the absorption process (Fig. 1).

The plot of the natural logarithm of the equilibrium pressure of hydrogen versus 1,000/T in which T is the absolute temperature in Kelvin allows us to understand that to equal equilibrium pressures will correspond very different temperatures when Cu–Li–Mg–H samples (with high initial content of $CuLi_{0.08}Mg_{1.92}$) are compared with MgH_2, $NiMg_2H_4$, or even with $Cu_2Mg + 3MgH_2$ [13]. Additionally, when the equilibrium pressure, at 200 °C, for a sample containing $CuLi_{0.08}Mg_{1.92}$–H is compared with

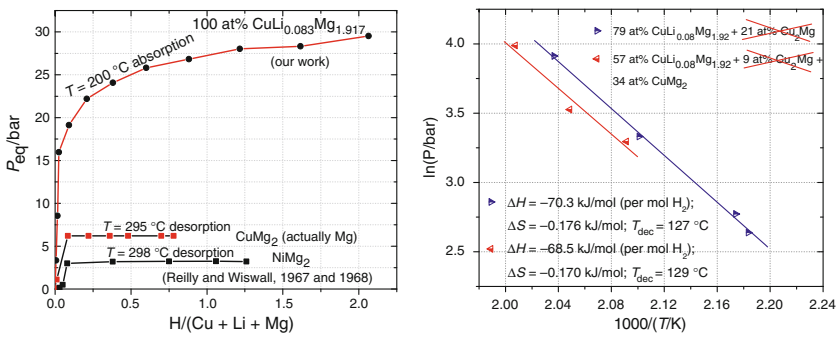

Fig. 1 *left* Absorption curve for a sample containing $CuLi_{0.08}Mg_{1.92}$ (considering that Cu_2Mg does not absorb hydrogen at 200 °C and at the referred pressures). *right* Natural logarithm of the equilibrium pressure versus 1,000/T for two samples with initial compositions (prior to hydrogen absorption) referred in the plot's legend

the equilibrium pressure of a sample containing $CuMg_2$, at 295 °C, the difference between plateau pressures can be higher than 21 bar [13] (Fig. 1). The latter means that $CuLi_{0.08}Mg_{1.92}$–H will release hydrogen at a much lower temperature.

Calculations of the decomposition temperature can be done, using:

$$G_{MH} - G_{H_2} = \Delta G = 0 \Leftrightarrow G^0_{MH} - G^0_{H_2} - R \cdot T \cdot \ln\left(\frac{P_{eq}}{P_0}\right) = 0 \quad (1)$$

$$\Delta G^0 = R \cdot T \cdot \ln\left(\frac{P_{eq}}{P_0}\right) = \Delta H^0 - T \cdot \Delta S^0 \quad (2)$$

$$\ln\left(\frac{P_{eq}}{P_0}\right) = \frac{\Delta H^0}{R} \cdot \frac{1}{T} - \frac{\Delta S^0}{R} \quad (3)$$

For

$$P_{eq} = P_0 \Rightarrow T_{dec} = \frac{\Delta H^0}{\Delta S^0} \quad \text{(per mol of } H_2\text{)} \quad (4)$$

in which G is the Gibbs energy, MH (metal-hydride), R the ideal gas constant, P_{eq} and P_0 is the equilibrium and atmospheric pressure, respectively, H^0 the enthalpy and S^0 the entropy when $P_{eq} = P_0$.

The previous calculations for the Cu–Li–Mg–H system lead to decomposition temperatures of 400 K (127 °C) for a sample containing – 79 at% of $CuLi_{0.08}Mg_{1.92}$ and 21 at% of Cu_2Mg– and of 402 K (129 °C) for a sample containing – 57 at% of $CuLi_{0.08}Mg_{1.92}$, 34 at% of $CuMg_2$ and 9 at% of Cu_2Mg. Cu_2Mg does not absorb hydrogen at the temperatures shown in Fig. 1.

Hydrides stability depends mostly on the enthalpy term (ΔH^0) as ΔS^0 is usually around -130 J (mol H_2)$^{-1}$ K^{-1}, which roughly corresponds to the H_2 molecule losing its translational degrees of freedom upon transformation from the gas phase into the solid state of the hydride. Nevertheless, in this system, ΔS^0 is higher than usually but still into the boundaries of the entropy of formation of the hydrides studied in the literature ($\Delta S(FeTi) \approx -0.104$ kJ/mol H_2 [14]; $\Delta S(LaNi_5) \approx -0.105$ kJ/mol H_2 [14]; $\Delta S(VH_2) \approx 0.141$ kJ/mol H_2 [14]; $\Delta S(PdH_{0.7}) \approx -0.098$ kJ/mol H_2 [14]; ΔS(CuLiMg–H) ≈ -0.170 kJ/mol H_2; $\Delta S(CuMg_2) \approx 0.138$ kJ/mol H_2 [15]; $\Delta S(NiMg_2) \approx -0.123$ kJ/mol H_2 [14]; $\Delta S(MgH_2) \approx -0.135$ kJ/mol H_2 [16]; $\Delta S(NaH) \approx -0.164$ kJ/mol H_2 [16]; $\Delta S(KH) \approx -0.169$ kJ/mol H_2 [16]; $\Delta S(UH_3) \approx -0.179$ kJ/mol H_2 [14]; $\Delta S(TiH_2) \approx -0.178$ kJ/mol H_2 [14]; $\Delta S(LiH) \approx -0.126$ kJ/mol H_2 [14]; $\Delta S(SrH_2) \approx -0.141$ kJ/mol H_2 [16]). ΔS^0 is mostly the responsible by the difference between the $Cu_2Mg + MgH_2$ and the $CuLi_{0.08}Mg_{1.92}$–H desorption temperatures.

For all of the hydrides to be discussed, ΔH^0 and ΔS^0 are negative, i.e., the hydrogenation reaction is exothermic and the dehydrogenation reaction is endothermic.

Inelastic neutron scattering

Time-of-flight (TOF) inelastic incoherent neutron scattering was collected at low temperatures at LANSCE, in FDS.

A sample with approximately –76 at% of $CuLi_{0.08}Mg_{1.92}$ and 24 at% of Cu_2Mg– was loaded with H_2 at 200 °C, at different pressures and loading times, before collecting a neutron vibrational spectrum (cycling treatments were performed over the same sample after each measurement. Between loadings, H_2 pressure was $\sim$1 bar and temperature dropped to room temperature). The sample was loaded: once for 1 h under 36 bar of H_2; twice for 6 h under 100 bar of H_2 and once for 21 h; once for 17 h and 25 min. and twice for 3 h (100 bar).

All data were collected at 10 K. Figure 2 shows the first Inelastic Neutron Scattering (INS) experiment in comparison with measurements of other samples of the same system – 33 at% of $CuLi_{0.08}Mg_{1.92}$, 35 at% of $CuMg_2$ and 32 at% of Cu_2Mg- and – 42 at% of $CuLi_{0.08}Mg_{1.92}$, 32 at% of $CuMg_2$ and 26 at% of Cu_2Mg- after being submitted to one hydrogenation cycle and of $NiMg_2H_4$. The latter hydride exhibits the same spectra whatever the hydrogenation treatment used or number of cycles. It seems that the lattice vibrations happen at similar wavenumbers possibly indicating a similar monoclinic structure comprising a $[CuH_4]^{3-}$ anion complex.

INS spectra show that cycling has a strong effect on structure and ion distribution. On the other hand, this effect on the structure can moreover be due to the loading time or to the waiting time (time the sample waited, at ambient pressure, before being measured). In other words, there

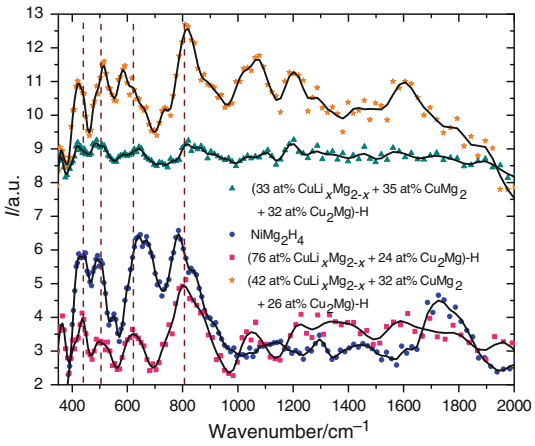

Fig. 2 INS results show similar spectra for different Cu–Li–Mg–H samples after one hydrogenation cycle. INS for $NiMg_2H_4$ is similar to the others spectra shown and does not depend of the hydrogenation process

might be a phase transition during hydrogen loading/releasing. These results show that during the first loading the structure was monoclinic with the Cu (bonded to H) ion probably occupying C_1 sites like in $[NiH_4]^{4-}$ in $NiMg_2H_4$ (monoclinic) [17], and that after 3 and 6 cycles the sample is likely to present a tetragonal structure similar to $CoMg_2H_5$ in which $[CoH_5]^{4-}$ occupies square-based pyramidal C_{4v} sites [18] or to present an extra phase with a tetragonal structure that can actually be MgH_2 [19] (Fig. 3).

Differential scanning calorimetry (DSC) and Thermogravimetry (TG)

Several samples were analysed by DSC/TG using a Netzsch instrument. Samples were heated from room temperature to 450 °C, at 5 and 10 °C/min. Alumina crucibles with lids were used at all times under high-purity argon gas flowing at 27 mL/min. Samples in the form of powder were hydrogenised before measured.

A literature search shows that MgH_2 in form of powder releases hydrogen in DSC instruments at temperatures that vary from the minimum of 325 °C [20] to a maximum of 433 °C [21] (Table 1). Although for MgH_2 the equilibrium desorption temperature (1–4) should be approximately 280 °C (553 K), in DSC the effect of kinetics counts as well, and therefore the lowest temperature found in the literature was 325 °C. Several DSC studies, that aimed to determine at which temperature MgH_2 releases hydrogen, were reported in the literature [20–28] (Table 1). Most of them focus on the effect of a catalyst on the desorption temperature of MgH_2.

One of the studies refers to nanoparticles of $CuMg_2$ [28]. $CuMg_2$ is hydrogenised to form MgH_2 and Cu_2Mg (5).

$$2CuMg_2 + 3H_2 \leftrightarrow Cu_2Mg + 3MgH_2 \quad (5)$$

According to Shao et al. [28] nanoparticles of $MgH_2 + Cu_2Mg$ will start releasing H_2 at 409 °C when the sample is at 4 MPa (40 bar) of H_2, while the equilibrium desorption temperature is 385 °C. The same study reports that Mg nanoparticles under the previous conditions desorb hydrogen at 472 °C (Table 1), while the equilibrium desorption temperature is 442 °C [28].

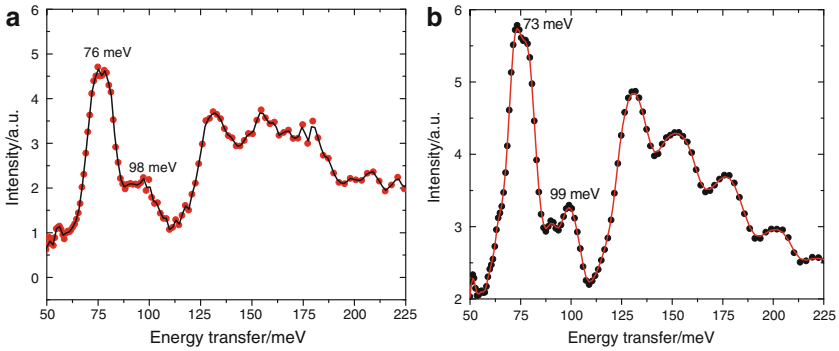

Fig. 3 **a** INS results show similar spectra for the third hydrogenation cycle for a Cu–Li–Mg–H sample (76 at% of $CuLi_{0.08}Mg_{1.92}$ and 24 at% of Cu_2Mg-loaded at 200 °C, twice for 6 h and once for 21 h under 100 bar of H_2). **b** INS spectra for MgH_2. After the first hydrogenation cycle results seem to indicate that MgH_2 is formed even in samples that do not contain $CuMg_2$

Table 1 Desorption temperature of MgH_2 (with tetragonal structure), obtained by means of DSC

Reference	Atmos.	Average particle size/milling conditions	Heating rate/°C min^{-1}	Desorption temperature/°C
[20]	Ar	Nano (20 h, Fritsch P7 planetary, 400 rpm, ball to powder weight ratio 40:1)	5	325
[21]	He	Nano (48 h, Fritsch P0 vibratory)	10	433
[21]	He	Nano (48 h, Fritsch P7 planetary, b–p–w–r 10:1)	10	372
[22]	Ar	7.9 nm	5	380
[23] (with 2% Co)	Ar	Order of μm (10 h, Spex planetary, b–p–w–r 3:1)	20	375
[24]	Ar	(15 h, Fritsch P5 planetary, b–p–w–r 15:1, 300 rpm)	5	330
[25]	Ar	(40 h, Kurimoto planetary, 885 rpm)	–	427
[26]	Ar	30 μm (10 h, Turbula planetary, b–p–w–r 10:1)	15	379
[27]	He	<100 nm (48 h, Fritsch P0 vibratory, b–p–w–r 20:1)	10	357
[28]	H_2 40 bar	300 nm	20	472 (Equilibrium temp. ~442 °C [28])
[28] (with Cu_2Mg)	H_2 40 bar	100 nm	20	409 (Equilibrium temp. ~385 °C [28])

In addition, the amount of desorbed hydrogen is not only related with the capacity of the hydride, its kinetics, grain size, possible catalysts added, but also with the way powders are milled [21]. Moreover, if the samples are not saturated, the amounts of released hydrogen cannot be compared or controlled.

Results show that hydrogenated samples containing $CuLi_{0.08}Mg_{1.92}$, start releasing hydrogen at $T < 50$ °C/323 K, then have a second release rate at around ~200 °C/473 K and finally a third release rate at about ~280 °C/553 K (Figs. 4 and 5). The first and second releases seem to be related with $CuLi_{0.08}Mg_{1.92}$–H and the third could be due to MgH_2 desorption. If this assumption is correct, this means that $CuLi_{0.08}Mg_{1.92}$–H will disproportionate into other hydrides.

Furthermore, if only $CuMg_2$ had contributed for the formation of MgH_2 (Fig. 4 mass losses and peaks at 282 and 287 °C), the maximum loss in weight percentage of the sample should be ~0.6 wt% since $CuMg_2$ is not present with more than ~23 wt%. The theoretical amount of hydrogen that can be released by $Cu_2Mg + 3MgH_2$ (5) is 2.6 wt% in a sample containing 100% of the mixture.

Likewise, if MgH_2 desorbs hydrogen at 282 °C, then the catalytic effect of $CuMg_2/Cu_2Mg$ is likely present and in addition a catalytic effect of $CuLi_{0.08}Mg_{1.92}$–H, since MgH_2 desorption temperature is 43 °C lower than the minimum temperature found in the literature for DSC experiments.

Hydrogen absorption experiments with nanostructured $CuMg_2$ samples, without activation process as in the case of this study, reveal that this compound will start absorbing hydrogen at ~250 °C [28]. All our samples absorbed hydrogen at 200 °C.

Using the total amount of hydrogen released by the sample during heating in Fig. 4 (left), the stoichiometry of $CuLi_{0.08}Mg_{1.92}$–H can be determined. Nonetheless, the absorption of hydrogen by $CuMg_2$ has to be taken into account, as well as the fact that Cu_2Mg will not absorb also hydrogenated at 200 °C. Samples do not seem to be saturated with hydrogen since they still present a peak corresponding to the parent's phase melting point (426 and 416 °C). Nonetheless, XRD patterns of the sample corresponding to the left curve have showed saturation

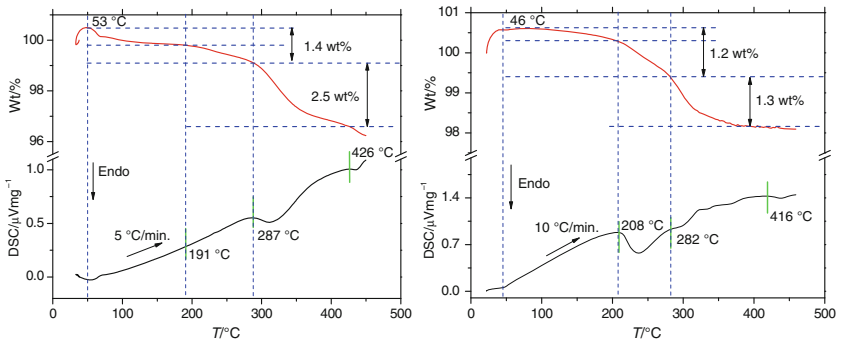

Fig. 4 DSC/TG curve of a sample containing 60 wt% of $CuLi_{0.08}Mg_{1.92}$, 28 wt% of $CuMg_2$ and 12 wt% of Cu_2Mg (62 at% of $CuLi_{0.08}Mg_{1.92}$, 28 at% of $CuMg_2$ and 10 at% of Cu_2Mg) that was hydrogenated at 200 °C and of a sample containing 69 wt% of $CuLi_{0.08}Mg_{1.92}$, 18 wt% of $CuMg_2$ and 13 wt% of Cu_2Mg (72 at% of $CuLi_{0.08}Mg_{1.92}$, 18 at% of $CuMg_2$ and 10 at% of Cu_2Mg) that was

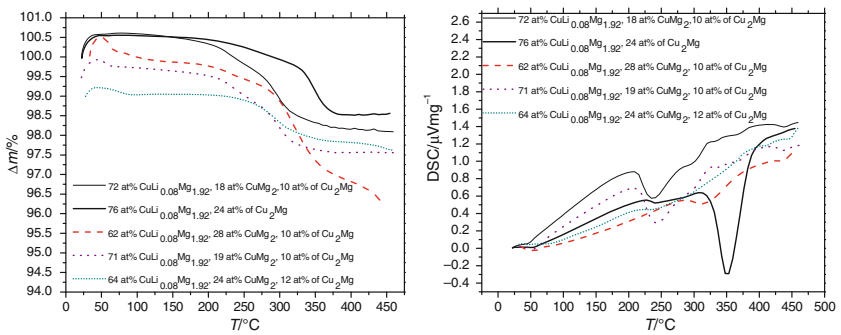

Fig. 5 DSC/TG curves of different samples from the Cu–Li–Mg–H system that prior from hydrogenation contained the phases and compositions signalized in the figures' captions. Samples were not saturated with hydrogen and suffered different hydrogenation cycles, at different pressures of H_2 and all at 200 °C. It can be observed a peak at low temperature ($T < 50$ °C), at approximately 208–220 °C, at 280–300 °C and finally the melting point of the parent $CuLi_{0.08}Mg_{1.92}$ at 420–426 °C

hydrogen at 200 °C. We have obtained a value of ~5.3 wt% that corresponds to $CuLi_{0.08}Mg_{1.92}H_6$ ($wt_H\% = 5.2\%$).

Ab initio calculations

Parent phase, $CuLi_{0.08}Mg_{1.92}$

Density Functional Theory (DFT) calculations with Projector Augmented Wave (PAW) pseudopotentials [29], as implemented in the Vienna Ab Initio Simulation Package code (VASP) [30–32], were performed. A plane wave cutoff of 355.18 eV, and k-spacings of $0.230 \times 0.230 \times 0.230$ Å^{-1} were used. Calculations were done in real space and were performed with P1 space group supercells containing 144 atoms (48 atoms of Cu, 96-n of Mg, and $n = 0$–12 of Li). The supercells contained as many atoms as possible to allow better approximations with the real Li concentrations (but such that the time spent on calculations were not completely impractical). Since $CuLi_xMg_{2-x}$ is a disordered structure, it had to be obtained by randomly substituting Mg by Li in several 6f Wyckoff positions (1/2, 0, z) or 6i Wyckoff positions (x, $2x$, 0) or in both positions within the supercells. The Generalized Gradient Approximation (GGA), and the Perdew–Burke–Ernzerhof (PBE) functional [33] were used, and no magnetic moments were included in the model. We have concluded that the stoichiometry that minimizes the energy of formation is $CuLi_{0.08}Mg_{1.92}$, which is in agreement with the experimental results [34]. Phonon calculations were also implemented and results of the phonon Density of States (DOS) are in agreement with the INS experimental results for the parent phase (Fig. 6).

Hydride phase, $CuLi_{0.08}Mg_{1.92}H_x$

Using DFT and the same conditions described for the parent phase (with one exception: we did not use supercells), several possible structures of $CuMg_2H_x$ were optimized. We did not replace Mg with Li because that would mean building a supercell and spend a large computational time. The goal was to obtain a starting point for further studies.

Therefore, since most of the hydrides are cubic structures or structures that can be considered as distortions of a cubic structure [17], we have started calculations with tetragonal and monoclinic structures, similar to that of the hydrides formed by the nearest neighbours of copper in the periodic table and Mg: $NiMg_2H_4$ and $CoMg_2H_5$ (e.g., $CuMg_2H_4$, as monoclinic C 2/c similar to $NiMg_2H_4$ structure—low temperature; $CuMg_2H_5$ as tetragonal P 4/nmm similar to $CoMg_2H_5$ structure). In Fig. 7 it can be observed that the most stable configuration corresponds to $CuMg_2H_5$ with a monoclinic C 2/c structure. Using this structure, we have built a supercell and replaced Mg atoms by Li atoms in three different sites of the initial configuration. The new optimized structure is even more stable ($\Delta E_f = -4$ kJ/mol of H_2).

Knowing what the most stable structure of the hydride is, is necessary, but not sufficient. To make a statement about what will be the reaction occurring upon hydrogen absorption more information is needed since the compound may disproportionate into other compounds/hydrides like in the case of $CuMg_2$. Nonetheless, when we compare these results with neutron diffraction [12] and inelastic neutron spectroscopy, we observe that it is highly possible that the first structure formed upon hydrogenation is a monoclinic one.

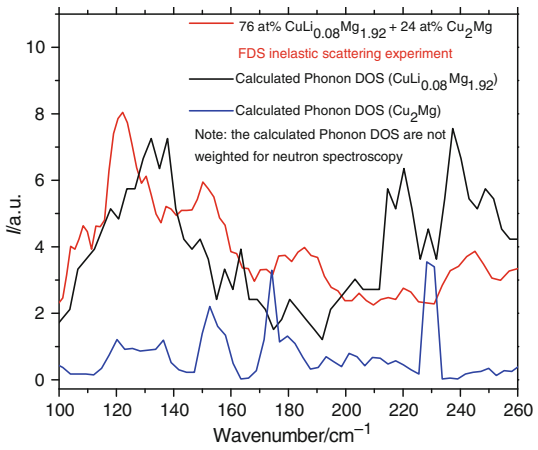

Fig. 6 Unweighted phonon DOS spectra, after ab initio, for the $CuLi_{0.08}Mg_{1.92}$ and Cu_2Mg crystal structures in comparison with the experimental INS spectrum of a sample containing both phases (without hydrogenation treatments)

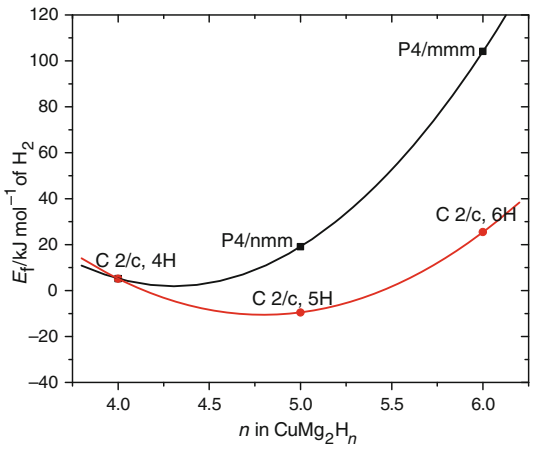

Fig. 7 Energy of formation of the hydride $CuMg_2H_n$ as a function of n (zero point energy was not included), for different types of crystal structures

Conclusions

After analysing the data obtained by hydrogen absorption, inelastic neutron spectroscopy, DSC/TG and first principles calculations we conclude that it is very likely that $CuLi_{0.08}Mg_{1.92}$ will react with hydrogen to form $CuLi_{0.08}Mg_{1.92}H_5$. Nonetheless, according to DSC's results, it is also possible that the stoichiometry of the product is $CuLi_{0.08}Mg_{1.92}H_6$.

The monoclinic C 2/c structure for the $CuLi_{0.08}Mg_{1.92}$ hydride (or a nearly derived structure) is in agreement with the results obtained both using neutron scattering techniques and first principles calculations.

Additionally, it can be concluded that even in samples that did not initially contain $CuMg_2$, it is clear the presence of MgH_2 formed after hydrogen uptake.

In this work it is also clear the roll of the Cu–Li–Mg–(H) as a catalyst for both $CuMg_2$ and MgH_2 during absorption and desorption.

Acknowledgements The authors would like to acknowledge Portuguese Science Foundation, FCT, for the project (PTDC/CTM/099461/2008 and FCOMP-01-0124-FEDER-009369). This work has benefited from the use of neutron scattering instrument FDS at the Lujan Center at Los Alamos Neutron Science Center, funded by DOE Office of Basic Energy Sciences. Los Alamos National Laboratory is operated by Los Alamos National Security LLC under DOE Contract DE-AC52-06NA25396.

References

1. Yang K, An JJ, Chen S. Influence of additives on the thermal behavior of nickel/metal hydride battery. J Therm Anal Calorim. 2010;102:953–9.
2. Fang KZ, Mu DB, Chen S, Wu F, Zeng XJ. Thermal behavior of nickel–metal hydride battery during charging at a wide range of ambient temperatures. Therm Anal Calorim. 2011;105:383–8.
3. Reilly JJ, Wiswall RW. The reaction of hydrogen with alloys of magnesium and copper. Inorg Chem. 1969;6(12):2220–3.
4. Braga MH, Ferreira J, Malheiros LF. A ternary phase in Cu–Li–Mg system. J Alloy Comp. 2007;436:278–84.
5. Hewat P. (2007) Inorganic Crystal Structure Database. 156880.
6. Schlapbach L, Zuttel A. Hydrogen-storage materials for mobile applications. Nature. 2001;414:353–8.
7. Braga MH, Ferreira J, Malheiros LF, Hamalainen M. HT-XRD on the study of Cu–Li–Mg Z. Kristallog suppl. 2007;26:299–304.
8. Orimo S, Nakamori Y, Eliseo JR, Zuttel A, Jensen CM. Complex hydrides for hydrogen storage. Chem Rev. 2007;107:4111–32.
9. Reilly J, Wiswall R. The reaction of hydrogen with alloys of magnesium and nickel and the formation of Mg_2NiH_4. Inorg Chem. 1968;7(11):2254–6.
10. Braga MH, Malheiros LF. WO2007046017.dp.
11. Match software, http://www.crystalimpact.com/match/Default.htm, Accessed 31 Aug 2011.
12. de Wolff PM, Visser JW. Absolute Intensities. Report 641.109. Technisch Physische Dienst, Delft, Netherlands. Reprinted Powder Diffract. 1988;3:202.
13. Braga MH, Acatrinei A, Hartl M, Vogel S, Proffen Th, Daemen L. New promising hydride based on the Cu–Li–Mg system. J Phys Conf Ser. 2010;251:012040.
14. Sandrock GD, Thomas G. IEA DOE SNL On-line Hydride Database. http://hydepark.ca.sandia.gov. Accessed 2009.
15. Andreasen A. Hydrogen storage materials with focus on main group I-II elements. PhD thesis. ISBN 87-550-3498-5; 2005.
16. Mueller WM, Blackledge JP, Libowitz GG, editors. Metal hydrides. London: Academic Press Inc; 1968.
17. Yvon K, Renaudin G. Hydrides: solid state transition metal complexes. Encyclopaedia of Inorganic Chemistry, 2006.
18. Parker SF, Jayasooriya UA, Sprunt JC, Bortz M, Yvon K. Inelastic neutron scattering, IR and Raman spectroscopic studies of Mg_2CoH_5 and Mg_2CoD_5. J Chem Soc Farad Trans. 1998;94(17):2595–9.
19. Schimmel HG, Johnson MR, Kearley GJ, Ramirez-Cuesta AJ, Huot J, Mulder FM. The vibrational spectrum of magnesium hydride from inelastic neutron scattering and density functional theory. Mater Sci Eng B. 2004;108:38–41.
20. Patah A, Takasaki A, Szmyd JS. The Effect of Cr_2O_3/ZnO on hydrogen desorption properties of MgH_2. Mater Res Soc Symp Proc. 2009:1148-PP03-38.
21. Balasooriya NWB. Poinsignon Ch. Preparation and characteristics of ball milled $MgH_2 + M$ (M = Fe, FeF_3 and VF_3) nanocomposites for hydrogen storage. Solid state ionics advanced materials for emerging technologies. Singapore: World scientific publishing Co. Pte. Ltd 2006. p 220–7.
22. Wu CZ, Wang P, Yao X, Liu C, Chen DM, Lu GQ, Cheng HM. Hydrogen storage properties of MgH_2/SWNT composite prepared by ball milling. J Alloys Comp. 2006;420(1–2):278–82.
23. Montone A, Grbovic J, Stamenkovic Lj, Fiorini AL, Pasquini L, Bonetti E, Antisari MV. Desorption Behaviour in Nanostructured MgH_2-Co. Mat Sci Forum. 2008;518:79–84.
24. Lillo-Rodenas MA, Aguey-Zinsou KF, Cazorla-Amoros D, Linares-Solano A, Guo ZX. Effects of carbon-supported nickel catalysts on MgH_2 decomposition. J Phys Chem C. 2008;112:5984–92.
25. Tessier P, Akiba E. Decomposition of nickel-doped magnesium hydride prepared by reactive mechanical alloying. J Alloys Comp. 2000;302:215–7.
26. Milovanovic S, Matovic L, Drvendzija M, Novakovic JG. Hydrogen storage properties of MgH_2-diatomite composites obtained by high-energy ball milling. J Micros. 2008;232(3):522–5.
27. Deledda S, Borissova A, Poinsignon C, Botta WJ, Dornheim M, Klassen T. H-sorption in MgH_2 nanocomposites containing Fe or Ni with fluorine. J Alloys Comp. 2005;404–406:409–12.
28. Shao H, Wang Y, Xu H, Li X. Preparation and hydrogen storage properties of nanostructured Mg_2Cu alloy. J Solid State Chem. 2005;178:2211–7.
29. Blochl PE. Projector augmented-wave method. Phys Rev B. 1994;50:17953–79.
30. Kresse G, Furthmüller J. Efficient iterative schemes for ab initio total-energy calculations using a plane-wave basis set. J. Phys Rev B. 1996;54:11169–86.
31. Kresse G, Furthmüller J. Efficient iterative schemes for ab initio total-energy calculations using a plane-wave basis set. Comp Mat Sci. 1996;6:1.
32. Kresse G, Joubert D. From ultrasoft pseudopotentials to the projector augmented-wave method. Phys Rev B. 1999;59:1758–75.
33. Perdew JP, Burke K, Ernzerhof M. Generalized Gradient Approximation Made Simple. Phys Rev Lett. 1996;77(18):3865–8.
34. Braga MH, Ferreira JJA, Siewenie J, Proffen Th, Vogel SC, Daemen LL. Neutron powder diffraction and first-principles computational studies of $CuLi_xMg_{2-x}$ ($x \cong 0.08$), $CuMg_2$, and Cu_2Mg. J Sol. Stat Chem. 2010;183:10–9.